References

[1] Reissner, E., "Finite Deflections of Sandwich Plates," *Journal of Aeronautical Sciences*, Vol. 15, July 1948, pp. 435-440.

[2] Wang, C. T., "Principle and Application of Complementary Energy Method for Thin Homogeneous and Sandwich Plates and Shells with Finite Deflections," NACA TN, 2620, 1952, pp. 1-33.

[3] Alwan, A. M., "Large Deflection of Sandwich Plates with Orthotropic Cores," *AIAA Journal*, Vol. 2, Oct. 1964, pp. 1820-1822.

[4] Wempner, G. A., and Baylor, J. L., "General Theory of Sandwich Plates with Dissimilar Facings," *International Journal of Solids and Structures*, Vol. 1, 1965, pp. 157-177.

[5] Sharifi, P., and Popov, E. P., "Nonlinear Finite Element Analysis of Sandwich Shells of Revolution," *AIAA Journal*, Vol. 11, May 1973, pp. 715-723.

[6] Nowinski, J. L., and Ohnabe, H., "Fundamental Equations for Large Delections of Sandwich Plates with Orthotropic Core and Faces," *Proceedings of 10th International Symposium on Space Technology and Sciences*, Tokyo, 1973, pp. 311-318.

[7] Berger, H. M., "A New Approach to the Analysis of Large Deflections of Plates," *Journal of Applied Mechanics*, Vol. 22, Dec. 1955, pp. 465-472.

[8] Iwinski, T., and Nowinski, J. L., "The Problem of Large Deflections of Orthotropic Plates (I)," *Archium Mechaniki Stosowanej*, Vol. 9, 1957, pp. 593-603.

[9] Nowinski, J. L., and Ismail, I. A., "Certain Approximate Analyses of Large Deflections of Cylindrical Shells," *Zeitschrift für angewandte Mathematik und Physik*, Vol. 15, 1964, pp. 449-456.

[10] Nash, W. A. and Modeer, J. R., "Certain Approximate Analyses of the Nonlinear Behavior of Plates and Shallow Shells," *Proceedings of Symposium on Theory of Thin Elastic shells*, Delft, 1959, Interscience, N.Y., 1960.

Incompressible Unsteady Flow through a Tube of Variable Cross-Section

D.P. Flemming*

Data Logic Canada Ltd., Ottawa, Ontario

A relationship connecting the rate of change of the volume flow rate of an inviscid incompressible fluid through a tube of varying cross-section with the pressure difference between two arbitrary cross-sections, should prove useful in hydraulic applications and has been used to simulate piston extrusion in a hypervelocity launcher.

The flow is assumed to take place through a uni-directional tube whos axis will be taken as the x axis, and whose cross-section area is given by a suitably differentiable quantity $A(x)$. In addition to incompressibility and zero viscosity, the absence of gravity and other body forces is assumed. While the varying cross-section area prevents the situation from being purely one-dimensional, we use the "quasi-one-dimensional" approach of Rudinger[1] assuming that: a) the column of fluid is long in relation to its cross-section, b) the cross-section area A is a slowly varying function of x.

The flow velocity u and the pressure, p, are thus assumed to be functions of x and the time t. To derive the relation under discussion† we use the Eqs. of conservation of mass and momentum:

$$(Au)_x = 0;\ Au = f(t) \tag{1}$$

$$u_t + uu_x + Vp_x = 0 \tag{2}$$

where V is the (constant) specific volume.
Thus

$$u_t = f'(t)/A(x) = -(\tfrac{1}{2}u^2)_x - Vp_x \tag{3}$$

Integrating (3) between 2 arbitrary cross-sections, x_1 and x_2, with t fixed, gives

$$f'(t)\int_{x_1}^{x_2}\frac{dx}{A(x)} = -\tfrac{1}{2}(u_2^2 - u_1^2) + V(p_1 - p_2)$$

$$= -\tfrac{1}{2}f(t)^2[A_2^{-2} - A_1^{-2}] + V(p_1 - p_2) \tag{4}$$

the subscripts 1 and 2 denoting values at x_1 and x_2, respectively. Solving (4) for $f'(t)$

$$f'(t) = \frac{V(p_1 - p_2) - \tfrac{1}{2}f(t)^2[A_2^{-2} - A_1^{-2}]}{\int_{x_1}^{x_2}\frac{dx}{A(x)}} \tag{5}$$

The previous Eq. has been found useful in the simulation of light gas hypervelocity launchers, specifically the simulation of the extrusion of a plastic piston, after reaching a region of decreasing cross-section area. While conditions a) and b) previously mentioned may not be satisfied, this approach was felt to give a reasonable approximation as part of the total launcher simulation.

Clearly Eq. (5) can be used to determine the piston motion from the pressures at its 2 ends. This in turn allows the use of the same Eq. for determining the pressure at intermediate points. The possibility of obtaining negative internal pressures should be born in mind. This would probably result in the longitudinal separation of the material.

Equation (5) might also be applied to transient problems in hydraulics. In the case of steady flow, in which $f'(t) \equiv 0$. Eq. (5) given the Bernouilli relation,

$$Vp_1 + \tfrac{1}{2}u_1^2 = Vp_2 + \tfrac{1}{2}u_2^2 \tag{6}$$

Reference

[1] Rudinger, George., *Wave Diagrams for Unsteady Flow in Ducts*, D.Van Nostrand, N.Y., 1955.

Received June 4, 1975; revision received September 25, 1975. This paper is based on research with which the author was associated while employed at the Defence Research Establishment Valcartier (formerly CARDE), Courcelette, Quebec, Canada. Their consent to its publication is gratefully acknowledged.

Index categories: LV/M Simulation; Hydrodynamics; Nozzle and Channel Flow.

*Consulting Analyst, Applied Sciences Group.

†The relation (equation (5)) is believed to have been originated by the late Mario Cloutier at DREV-who developed it for the light-gas gun application discussed below. The author is grateful to the Associate Editor for the particular derivation given here.

Numerical Investigation of Leading-Edge Vortex for Low-Aspect Ratio Thin Wings

Colmar Rehbach*

Office National d'Etudes et de Recherches Aerospatiales (ONERA), Chatillon, France

I. Introduction

FOR plane and cambered delta wings and for wings with curved leading edges exhibiting the well-known leading-edge vortex flow phenomenon,[1-5] we present theoretical results obtained by a singularities method.[6] These results are compared with flow visualizations performed in a water-tunnel.

Received June 23, 1975; revision received Oct. 21, 1975.

Index category: Subsonic and Transonic Flow.

*Research Scientist, Aerodynamics Department.

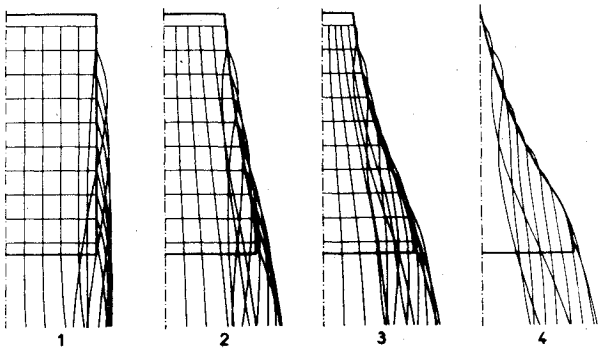

Fig. 1 Calculation of a wing with leading-edge separation by progressive deformation of a rectangular wing.

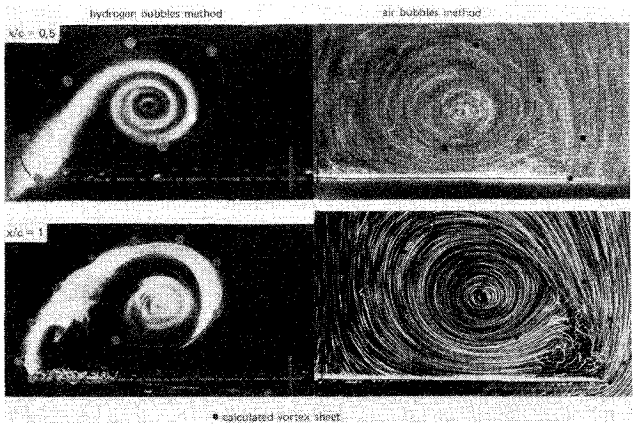

Fig. 2 Plane delta wing at 15° incidence.

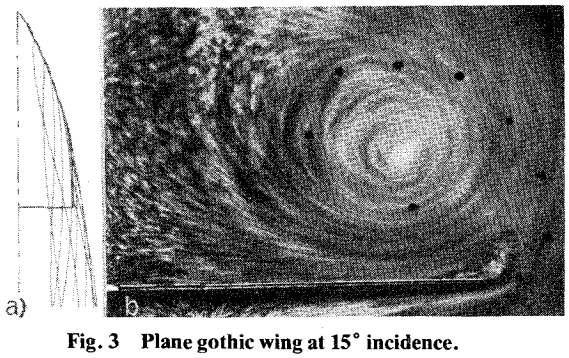

Fig. 3 Plane gothic wing at 15° incidence.

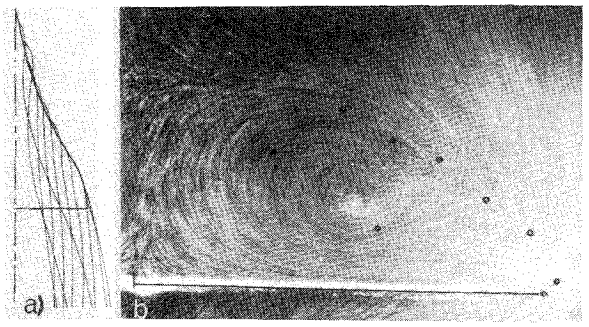

Fig. 4 Plane Concorde-type wing at 15° incidence.

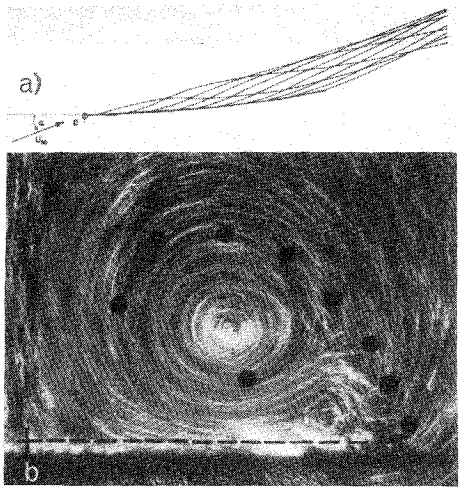

Fig. 5 Delta wing with concave upper surface at $\alpha = 15°$.

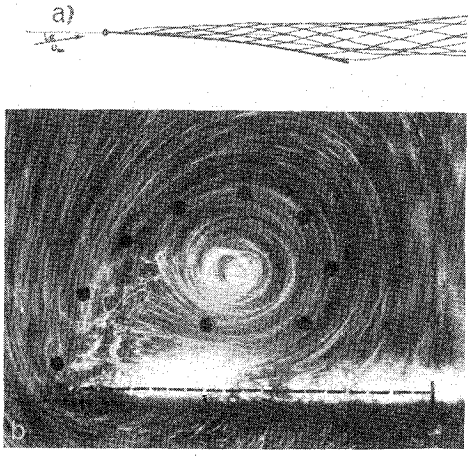

Fig. 6 Delta wing with convex upper surface at $\alpha = 15°$.

II. Some Particular Features of the Iteration Process

We recall that the unknowns of the discretized problem are the strengths of the concentrated vortices and the geometry of the sheet; both are interdependent, and the problem is nonlinear. The solution is to be obtained by an iteration procedure. The one that we use combines two well-known numerical methods[7,8] in order to improve the convergence. The details are given in Ref. 9.

Our first attempt, starting with an initial configuration involving a rough approximation of the leading-edge vortex sheet similar to that given in Ref. 10, was unsuccessful because of numerous difficulties in assuring the convergence. A convergent result finally was obtained by introducing an iteration cycle that performs a transformation of the wing planform and of its vortex sheet, thus enabling us to start the iteration process with a configuration presenting no leading-edge vortex sheet. This is illustrated in Fig. 1 for a thin uncambered wing of the Concorde type; we start with a rectangular wing whose vortex sheet is issued from the tips and the trailing edge only. A stepwise transformation of this initial wing leads to the desired planform. Five intermediate shapes are used to go from the rectangular wing to the Concorde-type wing; only two of them are shown on the figure.

III. Results

We first consider a plane delta wing with a semiapex angle 15° at an angle of attack of 15°. On Fig. 2 (right-hand side), calculated results are compared to flow visualizations by air bubbles (all of the experimental results shown here have been

obtained by H. Werle and M. Gallon in the ONERA water tunnel). The air bubbles in suspension in the water allow the visualization of the projections of trajectories in an arbitrarily chosen plane. The planes of observation shown here are the transverse planes perpendicular to the wing surface, and the first is located at 0.5 root chord from the apex, the second one at the trailing edge of the wing. The numerical results are represented by the intersection points of the vortex line with these transverse planes. Of course it is not possible to identify the bubbles that are issued from the leading edge, so that the comparison has only a qualitative character. However, the position of the experimental vortex core can be located easily on the photograph, which allows a check of the calculated sheet in an overall manner. Another experimental technique[11,12] has been used to visualize the vortex sheet itself. It uses hydrogen bubbles generated by electrolysis on the leading edge of the model. We show on the left-hand side of Fig. 2 the comparison of calculated and experimental results obtained by this technique in the same transverse planes as on the right-hand side. In the trailing edge plane, the agreement between experiment and calculation is good; in the midchord plane, on the contrary, there exists a noticeable discrepancy. In spite of some uncertainty in the visualized sheet contour due to the thickness of the model, the shape of the leading edge, the thickness of the illuminated slab of the flowfield, etc., this discrepancy should be attributed mainly to the imperfection of the numerical scheme: the real flow the rolling-up of the vortex sheet is already well established very close to the apex, whereas the numerical scheme does not take into account the apex as a singular point and leads to a vortex sheet that rolls up progressively as one moves in the downstream direction and as the number of vortex lines issued from the leading edge increases, thus providing a better representation of the sheet.

The next application concerns two plane wings with curved leading edges. The first one has a so-called gothic planform, and the second one has the Concorde-type planform of Fig. 1. Figure 3 shows the equilibrium position of the vortex sheet of the gothic wing at 15° incidence; Fig. 3a gives the projection in the $z=0$ plane of the calculated vortex sheet, and Fig. 3b gives the calculation-experiment comparison (air bubbles method) in the trailing-edge plane. A similar representation is used on Fig. 4 for the Concorde-type wing. Because of the qualitative character of the comparisons, we are not able to evaluate the accuracy with which the vortex sheet is determined. However, a good overall agreement with experiment is once more suggested by the position of the experimental vortex core, which is localized easily on the photographs. Besides, the character of the rolling-up, very different for these wings, is well reproduced by the numerical method.

The last example deals with two cambered untwisted delta wings with semiapex angle 15°. The projections in the $y=0$ plane of these wings (circular arcs) and of the equilibrium positions of their vortex systems are shown on Figs. 5a and 6a. The absolute value of the angle between the planes tangent to the apex and to the trailing edge is 12° for both wings; their incidences, measured with respect to the plane joining the apex to the trailing edge, are 15°. Thus the results obtained may be compared to those given for the plane delta wing (same incidence) so as to illustrate the effect on the vortex sheet contour of positive and negative camber. Figures 5b and 6b again show a good qualitative agreement between visualization (air bubbles method) and calculation in the trailing-edge plane.

In Fig. 7, we give the variation of the normal force coefficient with incidence for the plane delta wing, for which values obtained by other theories and by experiment are available. Our numerical results are compared to those of another numerical method,[10] to experiment,[13] and to three theoretical curves obtained within the limitations of slender-body theory: the first one for a wing without a leading-edge vortex sheet,[14] the second one for a wing with a leading-edge vortex sheet,[3] and the third one for a wing with a leading-edge vortex sheet calculated with the additional assumption of conical flow.[4] Our results are better than those obtained with a conical flow assumption[4] but appear to be less good than those of Ref. 10. The discrepancy is due, at least in part, to the difference in aspect ratio of the two wings (present wing $AR=1.07$; wing of Ref. 10 $AR=1$). Moreover, we found that the calculated pressure distribution compares poorly with experiment, especially as regards the pressure peak situated below the vortex core. Because of the highly singular character of the present numerical scheme based on finite strength discrete vortices, it does not seem possible to obtain much more accurate results by refining the vortex system, as some numerical tests have shown.

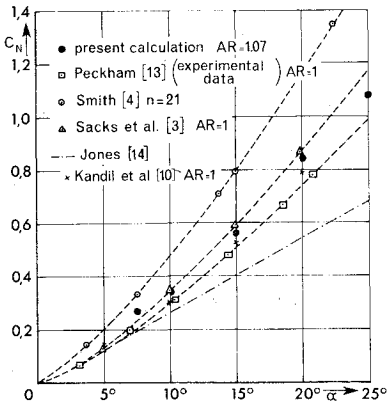

Fig. 7 Coefficient of normal force for a plane delta wing.

References

[1] Roy, M., "Caracteres de L'Ecoulement Autour d'une Aile en Fleche Accentuee," *Academie des Sciences (Paris), Comptes Rendus,* 1952, p. 2501.

[2] Legendre, R., "Ecoulement au Voisinage de la Pointe Avant d'une Aile a Forte Fleche aux Incidences Moyennes," *La Recherche Aeronautique,* Jan.-Feb. 1953.

[3] Sachs, A. H., "A Theoretical Investigation of the Aerodynamics of Slender Wing Body Combinations Exhibiting Leading Edge Separation," CR-719, March 1967, NASA.

[4] Smith, J.H.B., "Improved Calculations of Leading Edge Separation from Slender, Thin, Delta Wings," *Proceedings of the Royal Society (London),* Vol. A306, 1968, pp. 67-90.

[5] Legendre, R., "La Condition de Joukowski en Ecoulement Tridi-Mensionnel," *La Recherche Aerospatiale,* 1972, pp. 241-248.

[6] Rehbach, C., "Etude Numerique de Nappes Tourbillonnaires Issues d'une Ligne de Decollement pres du Bord d'Attaque," Rech. Aerosp. *La Recherche Aerospatiale,* 1973, pp. 325-330.

[7] Belotserkovskii, S.M., "Calculation of the Flow about Wings of Arbitrary Planform at a Wide Range of Angles of Attack," Library Transl. 1433, 1970, Royal Aircraft Establishment.

[8] Butter, D. J. and Hancock, G. J., "A Numerical Method for Calculating the Trailing Vortex System Behind a Swept Wing at Low Speed," *Aeronautical Journal,* Vol. 75, Aug. 1971, pp. 564-568.

[9] Rehbach, C., "Calcul d'Ecoulements Autour d'Ailes Sans Espaisseur Avec Nappes Tourbillonnaires Evolutives," *La Recherche Aerospatiale,* 1073, pp. 53-61.

[10] Kandil, O. A., Mook, D. T., and Nayfeh, A. H., "Nonlinear Prediction of the Aerodynamic Loads on Lifting Surfaces," AIAA Paper 74-503, 1974.

[11] Clutter, D. W., Smith, A. M. O., and Brazier, J. G., "Techniques of Flow Visualization Using Water as the Working Medium," Rept. ES 29075, April 1959, Douglas Aircraft Co.

[12] Thompson, D. H., "Visualization of Separated Flows in a Water Tunnel," TM ARL/A.266, March 1971, ARL, Melbourne, Australia.

[13] Peckham, D. H., "Low-Speed Wing Tunnel Tests on a Series of Uncambered Slender Pointed Wings with Sharp Edges," TR R&M 3186, 1961, Ames Research Center.

[14] Jones, R. T., "Properties of Low-Aspect-Ratio Pointed Wings at Speeds Below and Above the Speed of Sound," Rept. 962, 1950, NACA.